

Received September 2, 2021, accepted September 17, 2021, date of publication September 29, 2021, date of current version November 23, 2021.

Digital Object Identifier 10.1109/ACCESS.2021.3116704

# Giga-Bit Transmission Between an Eye-Safe Transmitter and Wide Field-of-View SiPM Receiver

WAJAHAT ALI<sup>1</sup>, GRAHAME FAULKNER<sup>1</sup>, ZUBAIR AHMED<sup>1</sup>, WILLIAM MATTHEWS<sup>1</sup>,  
AND STEVE COLLINS<sup>1</sup>, (Member, IEEE)

Department of Engineering Science, University of Oxford, Oxford OX1 3PJ, U.K.

Corresponding author: Steve Collins (steve.collins@eng.ox.ac.uk)

This work was supported by Engineering and Physical Sciences Research Council (EPSRC) Grant EP/R00689X/1

**ABSTRACT** In this paper, the performance of a wide field of view VLC receiver that includes a silicon photomultiplier (SiPM) is reported. In particular, a receiver field of view of  $\pm 45^\circ$  and On-Off keying data rates of 1.8 Gbps are demonstrated in 500 lux of ambient light. These results are achieved by combining optical absorption filters with a 6 mm by 6 mm SiPM. By absorbing ambient light between 450 nm and 750 nm these filters ensure that the SiPM is not saturated and reduces the transmitter power needed to support the required data rate. Unlike other optical filters the performance of absorption filters is not sensitive to angle of incidence. Consequently, the FOV is explained by a combination of the changes to the receiver's projected area, the path length of light in the filters and reflections from the filter surfaces. In addition, the results of the calculations, described by the IEC 62471:2006 safety standard, needed to determine the eye safety of a transmitter are reported. These calculations and the resulting irradiance levels available in a representative office scenario are used to show that data rates of more than 1 Gbps could be achieved with eye safe transmitters.

**INDEX TERMS** Visible light communications, silicon photomultiplier, optical wireless communications, colour glass absorptive filters, optical receivers, eye safe transmitters.

## I. INTRODUCTION

In the future Visible Light Communications (VLC) may complement existing Wi-Fi systems in some situations. The capacity of any future VLC channels will be determined by a combination of the channel's bandwidth and the signal to noise ratio (SNR) at the receiver's output. In most VLC systems, inexpensive photodiodes are the preferred photodetectors, however, the output noise from receivers that contain photodiodes is dominated by electronic noise in various components. The impact of this noise can be reduced by using an avalanche photodiode (APD) which uses avalanche multiplication to amplify the photocurrent. However, the avalanche process also generates excess noise that limits the best achievable SNR. Despite these limitations, the SNR and bandwidth of VLC systems are still good enough to support high-speed VLC WDM systems. For example, 15.73 Gbps

has been achieved at a distance of 1.6 m by using four different wavelengths [1]. Alternatively, a system employing beam steered, WDM and laser diodes could transmit 35 Gbps over a distance of 4 m [2]. Finally, WDM and polarization multiplexing have been combined to transmit 40.665 Gbps over 2 m [3]. However, all these VLC systems focused on the transmitter design to achieve higher SNR while their receivers provided a limited field of view (FOV).

Wide FOV receivers that support data rates of less than 1 Mbps have been described previously [4], [5]. However, designing a receiver with a wide FOV and the sensitivity and bandwidth required to support significantly higher data rates is a major challenge in the VLC systems. One way to increase the sensitivity of a receiver is to operate an APD above its breakdown voltage and placing it in series with a quenching device. As its name suggests the resulting single photon avalanche diode (SPAD) can detect single photons. However, after each photon is detected a SPAD requires several nanoseconds (known as the recovery or dead time)

The associate editor coordinating the review of this manuscript and approving it for publication was Fang Yang<sup>1</sup>.

to recharge so that another photon can be detected. The problems associated with this recovery time can be reduced by creating arrays of SPADs, generally referred to as Silicon photomultipliers (SiPMs). In addition, to reducing the impact of the recovery time another advantage of using SiPMs is that they can be significantly larger than other photodetectors with a similar bandwidth. These relatively large areas and the ability to detect single photons significantly reduces the irradiance needed by a VLC receiver. Consequently, when irradiance is used as the figure of merit a receiver that includes a SiPM is two orders of magnitude [6] better than a current state of the art optoelectronic integrated circuit containing an avalanche photodiode [7]. The lower irradiances required when a SiPM is used suggests that it may be possible to reduce the transmitter power so that high data rates can be achieved over a large coverage area with an eye safe transmitter.

Previously, the performance of SiPM receivers has been predicted [8]–[12] or determined experimentally [13]–[21]. The experimental results include transmitting 400 Mbps at a bit error rate (BER) of  $1.8 \times 10^{-3}$  to a custom-made 2.8 mm by 2.6 mm SiPM with an irradiance of  $1.4 \text{ mWm}^{-2}$  [17]. More recently, a commercially available 3 mm by 3 mm SiPM was used to achieve a data rate of 1 Gbps with a BER of  $10^{-3}$  at the same receiver irradiance [6]. However, the sensitivity of SiPMs to ambient light means that these results were obtained using narrow band-pass optical filters, which limit the Field of View (FOV) of the receiver [6], [19]. Subsequently, a data rate of 1 Gbps has been achieved in 500 lux of ambient light without these band-pass filters. However, without the filters this requires irradiances as high as  $55.7 \text{ mWm}^{-2}$  to achieve 1 Gbps [20].

In this paper, the eye safe transmitter powers for wavelengths between 400 nm to 750 nm, calculated using the methods described in the IEC 62471:2006 (photobiological safety of lamps and lamp systems) standard [22], are reported. In particular, the powers of transmitters that are not a photobiological hazard and are therefore classified as Risk Group 0 (exempt) are presented. The advantages of transmitting data using a wavelength of 405 nm are then highlighted. The irradiance at the receiver available from a set of the safest possible, exempt, transmitters in a typical office scenario is then determined for the first time. The irradiances in different parts of a representative office when these safe transmitter power limits are used are then calculated. To allow receivers containing SiPMs to support high data rates at these irradiances optical filters are required to reduce the amount of ambient light reaching the SiPM. Then, to avoid restricting the FoV of the receiver, different combinations of colour glass filters are considered. The irradiances from the transmitter required to support different data rates when the best filter combination and a large SiPM are used, are then determined. Finally, a method of predicting the FoV of a receiver that employs absorption filters is described and the data rates that can be supported in a representative office scenario are predicted.

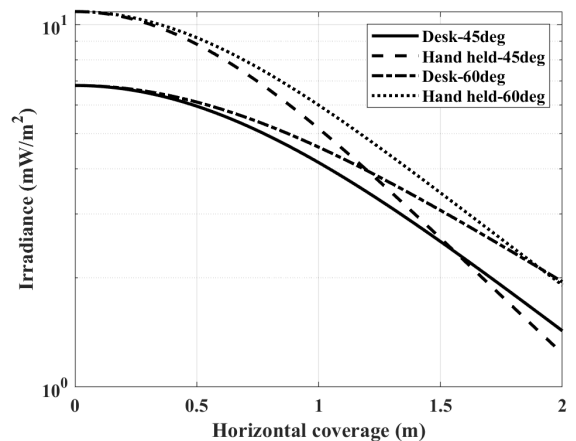


**FIGURE 1.** Irradiance as a function of different horizontal coverage with a receiver position at desk and when it is held by a user whilst standing considering  $45^\circ$  and  $60^\circ$  lambertian emitter.

The paper is organised as follows. Section II contains a description of an office scenario, a summary of the results of eye safety calculation at 405 nm and the irradiances available at some key locations in this office from eye safe 405 nm transmitters. The selection of the SiPM used in the receiver is then discussed in section III. This is followed in section IV by a description of the selection of the color glass filters used to reject ambient light. Section V then contains the results of experiments to determine the relationship between the irradiance from the transmitter at the receiver and the achievable data rate. The relationship between the angle of incidence of light from the transmitter and the fraction of this light reaching the SiPM is then explained in section VI. The results of the previous two sections are then used in section VII to predict the coverage in the office available from an eye safe 405 nm transmitter. Finally, conclusions are summarised in Section VIII.

## II. AN EXAMPLE OFFICE SCENARIO

The IEEE802.11bb task group on light communications provides details of different representative scenarios for VLC systems [23]. One of these scenarios, the enterprise scenario, envisages a 3 m high office with an area of 6 m by 6 m whose ceiling contains 9 access points (AP) arranged, in three rows, and separated from their nearest neighbours by 2.5 m. These locations mean that the maximum horizontal distance between a receiver and a vertical line from the centre of an AP is 1.77 m. Then the distance between an AP and a receiver (Rx) and the angle of incidence of light on a horizontal receiver both depend upon this horizontal distance and the height of the receiver from the floor. If the receiver is in a mobile phone next to the users ear it could be 1.7 m from the floor. However, when next to a user's ear any wireless link will only be required to support audio communications. In contrast, if a user is holding the device whilst standing, the receiver may be 1.3 m from the floor and a higher data rate may be required. At this height, the maximum distance between the closest AP and the Rx is 2.45 m and the angle

of incidence is  $46^\circ$ . Alternatively, if the receiver is located on the surface of a 0.85 m high desk then the maximum distance between the closest AP and the Rx is 2.78 m and the angle of the incidence is  $39^\circ$ . These results suggest that a receiver should have a field of view of at least  $\pm 45^\circ$ .

In addition to their relative position the irradiance at a receiver will depend upon the profile of the beam from the transmitter. Assuming that the beam profile can be represented by a Lambertian function then [24]:

$$\text{Irradiance}(d, \Phi) = \left( \frac{P}{d^2} \right) \left[ \frac{m+1}{2\pi} \right] \cos^m(\Phi) \quad (1)$$

where  $P$  is the transmitter's output power,  $\Phi$  is the angle between a line normal to the transmitter (Tx) and the line between the Tx and receiver (Rx) and  $d$  is the total distance between the Tx and the Rx. In addition if,  $\theta_{1/2}$  is the angle from the vertical at which the transmitter's power is half the maximum power then  $m = \ln(2)/\ln(\cos \theta_{1/2})$ .

The transmitters in VLC systems must be eye safe and ideally they should be in the safest possible risk group, which is Risk Group 0 (exempt). VLC transmitters may be required to irradiate an occupied space for long periods and the most relevant safety standard to evaluate these transmitters is the IEC 62471:2006 (photobiological safety of lamps and lamp systems) standard. Consulting this standard (Appendix) leads to the conclusion that, if the transmitter's dominant wavelength is 405 nm and  $\theta_{1/2} = 45^\circ$ , the maximum allowed power in the safest (exempt) risk group is 329 mW. However, transmitters emit a band of wavelengths and the results in Appendix A show that the maximum allowed power is sensitive to wavelength, with a minimum allowed power at 440 nm. If the spectrum of light from a particular transmitter is known the results in Appendix A could be used to determine the maximum allowed power for the particular transmitter. However, without this information it will be safer to restrict the power to the minimum allowed maximum power, which is 65.8 mW when  $\theta_{1/2} = 45^\circ$  and 98.7 mW, when  $\theta_{1/2} = 60^\circ$ . In addition to ensuring that the transmitter is exempt using these powers in calculations will underestimate the achievable data rates.

The irradiances at different horizontal distances between the Tx and the Rx from a 65.8 mW transmitter when  $\theta_{1/2} = 45^\circ$  or a 98.7 mW transmitter when  $\theta_{1/2} = 60^\circ$ , has been calculated using

$$\text{Irradiance}(d, \Phi, \psi) = \left( \frac{P}{d^2} \right) \left[ \frac{m+1}{2\pi} \right] \cos^m(\Phi) \cos(\psi) \quad (2)$$

where  $\psi$  is the angle of incidence with respect to the receiver axis. The results are shown in Fig 1 show that at the vertical heights of interest and the maximum horizontal distance the irradiance at the receiver is between  $1 \text{ mWm}^{-2}$  and  $2 \text{ mWm}^{-2}$ .

### III. SELECTION OF A SiPM

Previously, OOK data rates of up to 2.4 Gbps [6] and 3.45 Gbps [19] have been reported in 500 lux of ambient

**TABLE 1. Key parameters obtained from the manufactures data sheet for a j-series 60035 with an overvoltage of 5V [25].**

Parameter	60035
Number of Microcells	22292
Microcells active area diameter (( $\mu\text{m}$ ))	35
Fill factor (%)	75
Recovery Time constant (ns)	50
Photon Detection Efficiency (PDE) at 405 nm	0.5 (@ 6V)
Dark Count Rate (MHz)	5.5 (@ 6V)
Fast output pulse width (ns)	3

light when a 3 mm by 3 mm SiPM was used in the VLC receiver. The maximum photon detection efficiency of these SiPM occurs at 420 nm and in the range of wavelengths close to this maximum there is less ambient light at shorter wavelengths. These results were therefore obtained when data was transmitted by modulating the output from a laser diode with a central wavelength of 405 nm. However, the receiver used to support these data rates also included an optical filter with a 10 nm wide pass-band centred at 405 nm [19]. Unfortunately, the use of this optical filter restricts the field of view of the receiver to significantly less than  $\pm 45^\circ$ . The receiver's field of view can be increased by removing this filter. However, this exposes the SiPM to significantly more ambient light. Consequently, the irradiance from the 405 nm transmitter needed to support OOK data rates between 100 Mbps and 1 Gbps increases by a factor of 60. As a result, without a filter in 500 lux of ambient light, a 3 mm by 3 mm SiPM receiver could support a maximum data rate of 100 Mbps at the maximum irradiance in Fig. 1. A method of significantly reducing the impact of ambient light on the receiver is therefore required which allows the receiver to retain a wide field of view.

The impact of additional ambient light on the receiver's performance can be understood by considering the operation of a SiPM. A SiPM is an array of SPADs, known as microcells. When a photon creates an electron-hole pair in the active region of a microcell it can initiate an avalanche process which creates an output pulse. If these pulses are counted the result is a system that can detect individual photons. SiPMs therefore offer the opportunity to create VLC receivers whose performance is limited by Poisson noise, which is also known as shot noise. If the OOK bit error rate (BER) of a receiver is determined by Poisson noise then it can be calculated using

$$\text{BER} = \frac{1}{2} \left[ \sum_{k=0}^{n_T} \frac{(n_s + n_b)^k}{k!} \times e^{-(n_b + n_s)} + \sum_{k=n_T}^{\infty} \frac{n_b^k}{k!} \cdot e^{-n_b} \right] \quad (3)$$

where  $n_b$  is the number of detected photons per bit when a zero is being transmitted,  $n_s$  is the additional number of detected photons per bit when a one is transmitted and  $n_T$  is the decision threshold. The relationship between  $n_s$  and  $n_b$

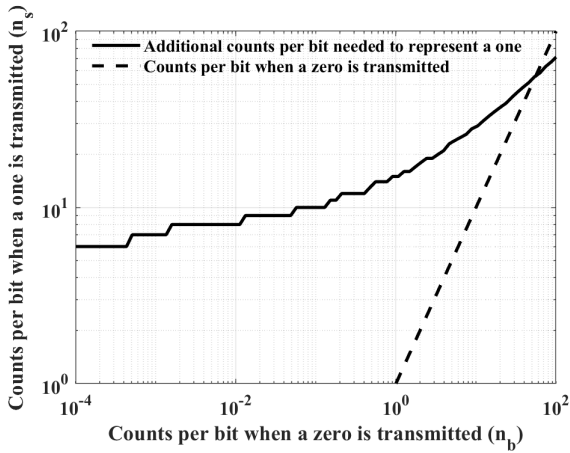


**FIGURE 2.** The number of additional counts per bit ( $n_s$ ) needed to distinguish a logic one from a logical zero when the number of counts per bit ( $n_b$ ) varies.

for a representative BER of  $10^{-3}$  is shown in Fig 2. The results in this figure show that  $n_s$  increases more slowly than  $n_b$ . Without the previously used optical filter in ambient light,  $n_b$  will be dominated by ambient light photons. This means that  $n_b$  will be proportional to the area of the SiPM. However, maintaining the BER will require a smaller increase in  $n_s$ . Consequently, increasing the area of the SiPM will reduce the irradiance from the transmitter needed to support a particular OOK data rate.

When selecting a SiPM for a VLC receiver SiPMs manufactured by ON-Semiconductor have been preferred because they have fast output pulses that increase the OOK data rate at which the SiPM causes inter-symbol interference [25]. Based upon the results in Fig. 3, experiments have been performed with the largest ON-Semiconductor SiPM, which is a J series 60035 SiPM, whose parameters are listed in Table 1. The full-width at half maximum of the fast output of this SiPM, is 3 ns, which corresponds to an exponential time constant ( $\tau$ ) of 1.36 ns. The 3 dB bandwidth created by an exponential decay with a decay time  $\tau$  is

$$f_{3dB} = 1/(2\pi\tau) \tag{4}$$

which means that the bandwidth of the fast output pulses of this SiPM is 116 MHz.

In addition to determining the background count rate a potentially more significant impact of ambient light on a SiPM is that it might saturate the SiPM's response. SiPM saturation arises because each avalanche event has to be quenched. The SiPMs manufactured by ON-Semiconductor employ a passive quenching mechanism to reduce the bias voltage across the microcell to less than its breakdown voltage. This halts the avalanche event but the quenched microcell must then be recharged and during this recovery time the microcell's photon detection efficiency (PDE) is reduced. At high photon fluxes the average time between photons arriving at a microcell can be shorter than the recovery time. Consequently, at high photon fluxes the probability that

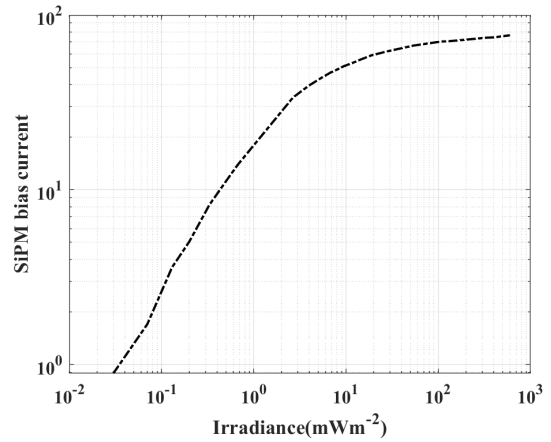


**FIGURE 3.** 60035 SiPM bias current at various irradiances 405nm light.

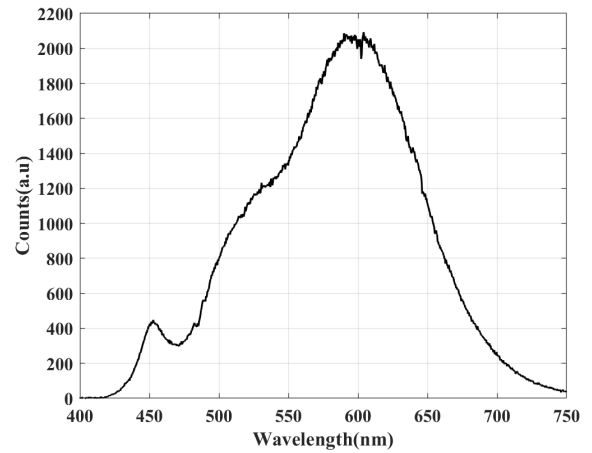


**FIGURE 4.** White LED spectrum from the 8W philips IBRS 10461 domestic lighting bulb used as background illumination.

a photon will be detected reduces until the rate at which photons are detected saturates.

The charge needed to recharge the capacitance of each microcell is provided by the voltage source that biases the microcells above their breakdown voltage. Since all the microcells are identical the current required to maintain the SiPM bias voltage is proportional to the rate at which photons are detected. Consequently, measuring this 'bias current' when the SiPM is irradiated with varying amounts of light is a convenient way of observing saturation [6].

The bias current required by a 60035 SiPM has been measured as the irradiance from a 405 nm laser diode was varied using a polariser placed in front of the laser diode. The results in Fig. 3 show the expected linear response at low irradiances followed by a non-linear response and eventually saturation. A comparison of the expected irradiance values in Fig 1 and these results shows that the irradiance from the transmitter alone forces this SiPM to operate in the non-linear response region between  $1 \text{ mWm}^{-2}$  and  $11 \text{ mWm}^{-2}$ . More importantly, exposing the SiPM to 500 lux of the ambient light

**TABLE 2.** SiPM bias currents with different combinations of filters.

Filters on the receiver with GG420 on the wLED	Bias Current
No Filter	72.0 mA
One BG3 filter	55.4 mA
Two BG3 filters	48.8 mA
Two BG3 filters and a BG39 filter	35.5 mA
Two BG3 filters, a BG39 filter and a Hoya B370 filter	14.3 mA

from a 8W Philips IBRS 10461 saturated the bias current. The SiPM must therefore be protected from ambient light using optical filters.

**IV. FILTER SELECTION**

The impact of using different filters to reduce the amount of ambient light reaching the SiPM has been assessed by measuring the SiPM bias current. Unlike the interference filters used previously with SiPMs in VLC receivers absorption filters have a wide FoV. The spectrum of light from a warm white LED in Fig 4 shows that filters are required to absorb wavelengths from as close to 405 nm as possible to wavelengths longer than 750 nm. Unfortunately, none of the available filters are ideal for this application and so different combinations of absorption filters have been considered.

In addition to protecting the SiPM from ambient light any filter should have the minimum possible impact on the light reaching the SiPM from the transmitter. One way that this can be achieved, without having a significant impact on the ambient light, is to place a GG420 filter in front of the white LED to block wavelengths shorter than 420 nm. In front of the IBRS 10461 the SiPM bias current is 72 mA. The results in Fig. 3 show that under these conditions the SiPM is saturated.

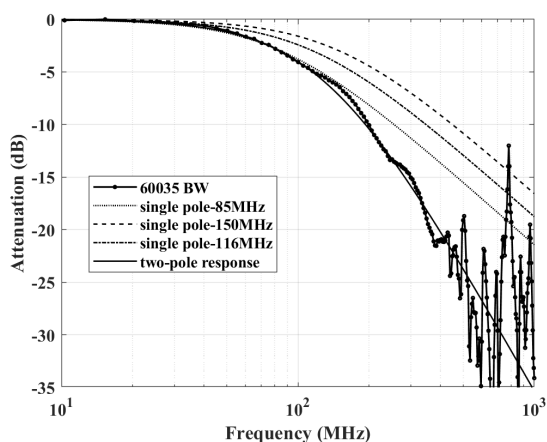


**FIGURE 5.** The frequency response of the VLC link.

A Schott glass BG3 filter, which transmits 76% of the incident 405 nm light and less than 10% of light between 490 nm and 690 nm, reduces the bias current from 72 mA to 55.4 mA. Adding a second BG3 filter then reduces this again to 48.8 mA, which is equivalent to an irradiance from

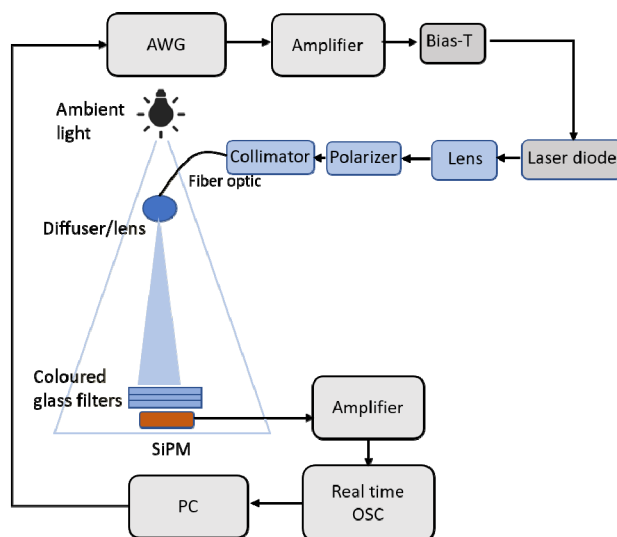


**FIGURE 6.** Schematic of the experimental setup used to perform data transmission using SiPM and color glass filters. The distance between the transmitter and receiver was 35 cm.

the 405 nm transmitter of  $10 \text{ mWm}^{-2}$ . The spectrum of the ambient light transmitted through these filters showed significant components at wavelengths shorter than 470 nm and longer than 700 nm. A BG39 filter, which transmits 87% of the light at 405 nm whilst transmitting less than 10% of the light at wavelengths longer than 660 nm, was therefore added to the two BG3 filters. This reduced the SiPM bias current to 35.5 mA. The only ambient light transmitted through these three filters was at wavelengths shorter than 470 nm. A Hoya B370 filter, whose transmission is less than 15% of the light between 450 nm and 700 nm was therefore added to the other filters which reduced the bias current to 14.3 mA. Although, this filter only transmits 67% of any light at 405 nm its use means that the SiPM is operating in its linear region.

**V. DATA TRANSMISSION EXPERIMENTS**

Experiments to determine the performance of a receiver that incorporates a 60035 SiPM in the presence of filtered ambient light have been performed using the set up shown in Fig. 6. The laser diode used in these experiments was a Thorlabs L405P20 with a peak wavelength of 405 nm. This laser diode was biased at 35.5 mA using a laser driver and a bias-T ((ZFBT-4R2GW+) was used to add a modulating signal to this DC bias. This signal was itself generated by a 10 GHz Tektronix Arbitrary Waveform Generator (AWG) and amplified by a 6 GHz (FMAM3269, 10 MHz to 1 GHz) amplifier to produce a 1.7 V peak-to-peak signal. The resulting modulated light from the laser diode was coupled to an optical fiber through a wire grid polarizer and a collimator. A lens and a diffuser were then used at the other end of fiber to create a uniformly illuminated area in which the receiver was placed. During experiments the polarizer in the setup was used to vary the irradiance across this area.

The receiver used in the experiments consisted of a SiPM, enclosed in a box so that the SiPM was only exposed to

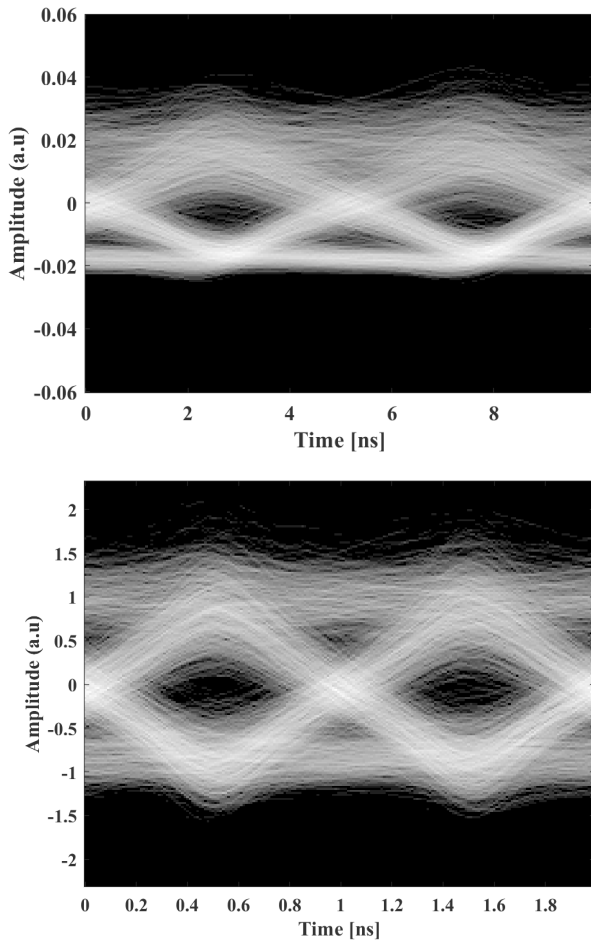


**FIGURE 7.** Eye diagrams with the best combination of filters under 500 lux of ambient light (top) 200 Mbps with a BER of  $10^{-3}$  without DFE (bottom) 1 Gbps with a BER of  $10^{-3}$  with DFE.

light entering via an aperture and any filters placed over the aperture. A bias voltage of 28 V was applied to the SiPM and its fast output was connected to a ZFL-1000LN+ 1 GHz amplifier whose output was captured by a Tektronix MSO64 oscilloscope (4 GHz, 25 GS/s).

Before data transmission experiments were performed the frequency response of the VLC link was measured by replacing the AWG and oscilloscope in this experimental set-up with a HP-8712 network analyser. The results in Fig. 5 show that the link's frequency response approximates a single pole response, with a 3 dB bandwidth of 85 MHz, up to 150 MHz and then deviates from this behaviour. The response was more accurately modelled using the product of two single pole responses, with 3 dB frequencies of 116 MHz and 150 MHz. As explained earlier, the pole at 116 MHz was created by the 3 ns fast output pulses and was therefore expected. The origins of the second pole are unknown. However, the two poles mean that the VLC link has a 3 dB frequency of 85 MHz. Since this is smaller than the expected 3 dB frequency, the unexplained 150 MHz pole, means that the results obtained in these experiments will under-estimate the performance of the SiPM receiver.

The OOK data rate that can be transmitted across this VLC link has been determined using the AWG to generate a pseudorandom binary sequence (PRBS) OOK signal. To accommodate the 10 MHz high pass response of the ZFL-1000H+ amplifier 8b10b encoding was used. The resulting receiver output signal was sampled at a rate of 6.25 samples per bit and then post-processed in MATLAB®. In particular, to reduce noise in the signal it was low-pass filtered using a 6<sup>th</sup> order Butterworth filter with a bandwidth of 0.7 times the data rate. The resulting analog signal was then synchronized with the transmitted signal and sampled at the middle of each bit. When needed DFE was applied to this down sampled signal. Finally, the threshold used to distinguish between transmitted ones and zeros was optimised to minimise the bit error rate when 10 different sequences of  $2^{15}$  pseudo-random bits were transmitted across the link. To replicate conditions that might be encountered when the receiver is used in an indoor down-link the receiver was also illuminated by 500 lux from the warm white LED (6W+ 8W Philips IBRS 10461), whose spectrum is shown in Fig. 4. The results in Table 2 show that adding a HoyaB370 filter to two BG3 filters and a BG39 filter at the receiver reduced the impact of ambient light on the receiver. However, it also has a significant impact on the amount of 405 nm light reaching the receiver. The impact of this filter on the receiver's performance was therefore determined by measuring the irradiance required to transmit 1 Gbps with a BER of  $10^{-3}$  to the receiver. With DFE but without the HoyaB370 filter the average irradiance from the transmitter at the receiver needed to support 1 Gbps was  $2.8 \text{ mWm}^{-2}$ . In contrast, although the HoyaB370 filter only transmits 67% of the light at 405 nm, when this filter was added to the receiver, the same data rate and BER required an irradiance at the receiver of only  $1.83 \text{ mWm}^{-2}$ . The Hoya filter therefore reduces the irradiance from the transmitter required to support 1 Gbps and it is therefore part of the best combination of filters.

The performance of a receiver containing a 60035 and the best combination of filters has been investigated in more detail. The OOK data rates with a BER of  $10^{-3}$  that could be transmitted at different average irradiances from the transmitter at the front of the receiver filters in the presence of 500 lux of ambient light are shown in Fig 8. The results in this figure clearly show that without DFE this receiver has a maximum data rate of approximately 400 Mbps, which is approximately four times the bandwidth of the SiPM. However, with DFE the maximum data rate increases to 1.8 Gbps.

A BER of  $10^{-3}$  is smaller, and hence more difficult to achieve, than the BER of  $3.8 \times 10^{-3}$  which is often used to characterise the performance of VLC systems [1], [19]. Some users may prefer to avoid using a GG420 filter on the ambient light sources. The performance of the receiver has therefore been determined at a BER of  $3.8 \times 10^{-3}$  with the GG420 in place and with it removed. As shown in Fig 8, removing the GG420 filter and accepting a BER of  $3.8 \times 10^{-3}$  coincidentally leads to results that are very similar to the

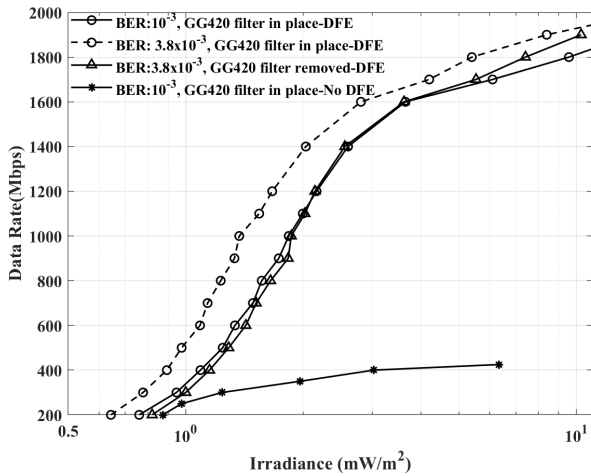


**FIGURE 8.** OOK data rate as a function of the irradiance from the transmitter with bit error rates of  $10^{-3}$  and  $3.8 \times 10^{-3}$  with the GG420 in place and with a BER of  $3.8 \times 10^{-3}$  with the GG420 removed from the white LED.

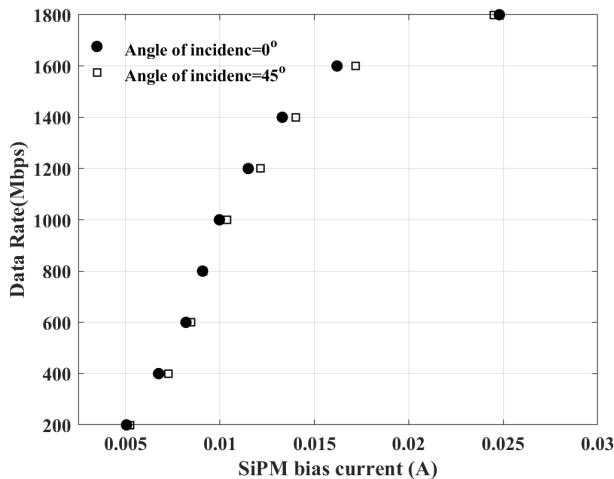


**FIGURE 9.** The data rates achieved at different angles of incidence at various SiPM bias currents.

results obtained with the filter in place and a BER of  $10^{-3}$ . This filter can therefore be removed if this higher BER is acceptable. Alternatively, the results in Fig 8 also show that retaining this filter and accepting the higher BER leads to an increase in the data rates that can be supported at lower irradiances. For example, at approximately  $1.4 \text{ mWm}^{-2}$  placing the GG420 filter over the WLED increases the data rate that can be transmitted from 600 Mbps to 1 Gbps.

### VI. IMPACT OF CHANGING ANGLE OF INCIDENCE

The motivation for using absorption filters is to avoid restricting the field of view of the receiver. Experiments have therefore been performed with light from the 405 nm transmitter reaching a SiPM covered by two BG3 filters, a HoyaB370 and a BG39 at an angle of incidence of  $45^\circ$ . The experimental results obtained in this orientation and when the angle of incidence is zero degrees, are shown in Fig 9. The results in

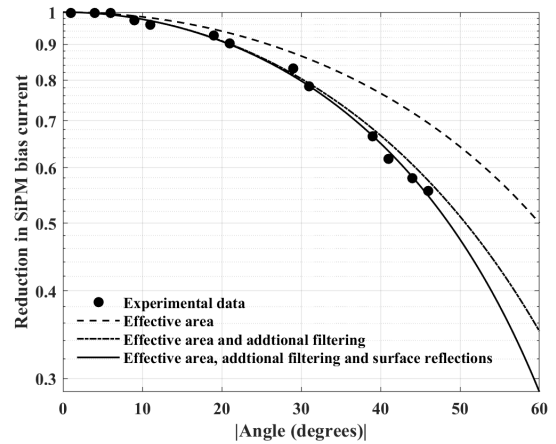


**FIGURE 10.** The reduction in SiPM bias current at various angles of incidence. The experimental data is shown as dots, whilst the different contributions to the variation of SiPM bias current with angle are shown as lines.

this figure show that, as expected, each data rate requires the same irradiance from the transmitter on the receiver surface and hence the same SiPM bias current.

The relationship between the irradiance from the transmitter reaching the front of the receiver’s filters and the irradiance on the SiPM surface will depend upon the angle of incidence. The irradiance of 405 nm light reaching the SiPM with the best combination of filters has therefore been measured at different angles of incidence. In these experiments the receiver was placed on a Melles Griot rotational stage and aligned to the transmitter when the angle of rotation was zero degrees. The polariser was then adjusted so that the irradiance falling on the receiver,  $0.21 \text{ mWm}^{-2}$ , was low enough to ensure that the SiPM bias current was proportional to the irradiance on the SiPM’s surface. The receiver was then rotated to change the angle of incidence of the light and the SiPM bias current at each position was measured using a Keithley 195 digital multi-meter. In order to confirm that the receiver was accurately aligned to the transmitter the angle of incidence was varied in both directions. A small asymmetry in the measured bias currents showed that the orientation of the SiPM within the receiver created a misalignment of  $1.5^\circ$  between the angle of rotation and the angle of incidence. Once this is taken into account the measured SiPM bias currents, shown in Fig. 10 had the expected dependence on the modulus of the angle of incidence. Three phenomena contribute to the reduction in the 405 nm irradiance reaching the SiPM, and hence the SiPM bias current, observed in Fig. 10. The first of these is the effective area of the SiPM,  $A_{\text{eff}}$ , which at an angle of incidence  $\theta_{\text{inc}}$ , is given by

$$A_{\text{eff}} = A \cdot \cos(\theta_{\text{inc}}) \tag{5}$$

where A is the area of the SiPM.

The second phenomenon contributing to the reduction in SiPM bias current is the increase in the path length through the absorption filters. If the effective attenuation coefficient

of the filters at 405 nm is  $\alpha$  then the transmission coefficient is

$$T(\theta_{inc}) = \exp(-\alpha t / \cos(\theta_f)) \quad (6)$$

where  $t$  is the thickness of the filter and Snell's Law means that  $\cos(\theta_f)$  is

$$\cos(\theta_f) = \sqrt{1 - (n_{air} \sin(\theta_{inc}) / n_{filter})^2} \quad (7)$$

where  $n_{air}$  and  $n_{filter}$  are the refractive index of air and the filter respectively. The final phenomenon which contributes to the reduction in SiPM bias current is reflections from the surfaces of the filters and the SiPM itself. The impact of these reflections on the light transmitted through each surface can be calculated using the Fresnel equations [26].

The experimental data and the angle dependence arising from the changes in the effective area of the SiPM are both shown in Fig. 10. The results in this figure shows that the irradiance on the SiPM is more sensitive to angle than the effective area. The impact of a combination of the effective area and the extra path length in the filters has been calculated by multiplying (5) by (6). The impact of (6) depends upon the value of  $\alpha t$ , which can be calculated using

$$\alpha t = -\ln(T(0)) \quad (8)$$

where  $T(0)$  is the transmission coefficient of the combination of filters at 405 nm when the angle of incidence is zero. The measured transmission coefficient of the combined filters at this wavelength is 0.31 and hence  $\alpha t = 1.2$ . The results in Fig 10 show that with this parameter the combination of the extra path length and the effective area explains the angle dependence of the SiPM bias current at smaller angles. However, it slightly under estimates the angle dependence at angles larger than approximately  $40^\circ$ . At larger angles reflections from the surfaces of the filters and encapsulation of the SiPM, increase. The impact of these reflections has been estimated by assuming that the refractive index of the filters and the encapsulation is 1.5. The results in Fig. 10 show that the three phenomena explain the angle dependence of the observed data.

### VII. COVERAGE WITH 60035 SIPM

Equations (5) to (8) have been used to predict the irradiance reaching the SiPM through the best filter combination from a Lambertian transmitter on two horizontal planes in the enterprise scenario. With a 3 m high ceiling, one of these horizontal planes, representing the surface of a desk, is 2.15 m below the ceiling. Whilst the other plane, represents the possible locations of a hand held device.

The results in Fig 11 shows the predicted data rates for a Lambertian transmitter with a beam divergence of either  $\pm 45^\circ$  or  $\pm 60^\circ$  when a GG420 filter is not used. In each case the transmitter power is assumed to be a conservative estimate of the maximum power allowed from an exempt (Risk Group 0) transmitter. The results in Fig. 11 are shown to a maximum horizontal distance of 2 m, which corresponds to a spacing between transmitters of 2.8 m. Consequently, this

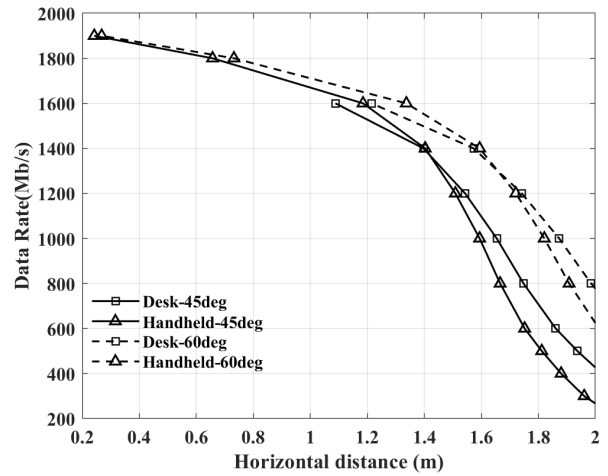


**FIGURE 11.** Predicted data rates from a single transmitter with a BER of  $3.8 \times 10^{-3}$  as a function of horizontal distance. These results were obtained using conservative estimates of the maximum powers from an exempt transmitter, 65.8mW and 98.7mW for beam divergences of  $\pm 45^\circ$  and  $\pm 60^\circ$  respectively.

figure can be used to estimate the minimum achievable data rate for different distances between transmitters. For example, if the transmitters are spaced by 2.5 m in two directions as in section II, the maximum horizontal distance between the transmitter and the receiver is 1.77 m. If the transmitters beam divergence is  $\pm 45^\circ$  the minimum achievable data rates are approximately 800 Mbps on a desk and 600 Mbps for a hand held device. However, if the divergence from the transmitter is  $\pm 60^\circ$  the corresponding data rates are 1.15 Gbps and 1.1 Gbps. Alternatively, if a GG420 filter is placed over the WLED the minimum data rates for a  $\pm 45^\circ$  transmitter increased to 1.15 Gbps and 1.0 Gbps on the two planes and 1.4 Gbps on both planes with a transmitter divergence of  $\pm 60^\circ$ .

### VIII. CONCLUSION

To provide the required quality of service all parts of an occupied space, for example an office, need to be illuminated by one or more VLC transmitters. Consequently, the risk group of VLC potential transmitters has been determined using the IEC 62471:2006 (photobiological safety of lamps and lamp systems) international standard. The results for extended light sources show that wavelengths near 400 nm are less hazardous than slightly longer wavelengths. Furthermore, if the beam from the transmitter is Lambertian, conservative estimates of the maximum power allowed at 405 nm in the lowest risk group are 98.7 mW ( $\theta_{1/2} = 60^\circ$ ) and 65.8 mW ( $\theta_{1/2} = 45^\circ$ ). When used in a representative office scenario described in section II this latter power would lead to irradiances between  $11 \text{ mWm}^{-2}$  and  $1 \text{ mWm}^{-2}$ . In addition, this scenario suggests that any receiver should have a field of view of at least  $\pm 45^\circ$ .

An advantage of using SiPMs is that they can detect individual photons. The Poisson statistics that determine the



performance of the resulting photon counting receiver mean that the number of detected photons from the transmitter required to support a particular data rate depends upon the number of ambient light photons detected by the SiPM. However, using a larger SiPM will reduce the required irradiance from the transmitter needed to support a particular data rate. The transmitter irradiance required to support a particular data rate can be reduced further by using filters to protect the SiPM from ambient light.

A second benefit of using optical filters in conjunction with a SiPM occurs because SiPMs have an unavoidable non-linear relationship between the irradiance falling on them and their output. To reduce the required transmitter irradiance, without severely limiting the receiver's field of view, absorption filters have been used as part of a VLC receiver.

The combination of absorption filters used in the receiver were selected based on their transmission probability at 405 nm and their impact upon the SiPM's bias current in ambient light. Subsequently, results of data experiments showed that, as predicted from Poisson statistics, even filters that attenuate the transmitter's wavelengths can improve the performance of the receiver. Other results showed that with the best combination of filters, a large SiPM and DFE it is possible to achieve a data rate of 1.8 Gbps in 500 lux of ambient light.

Results have been presented with angles of incidence of  $0^\circ$  and  $45^\circ$  that confirm that the data rate that can be supported by a SiPM depends upon the irradiance of light from the transmitter reaching the SiPM surface. In addition, the irradiance from the transmitter reaching the SiPM at different angles of incidence has been explained in terms of a combination of projected area, increased absorption in the filters and reflections from the filter surfaces. These results and the measured data rates under different conditions have been combined to predict the data rate that can be supported in an example office scenario. These results show that in this scenario it will be possible to support OOK data rates of more than 1 Gbps with low power 405 nm transmitters. The fact that these transmitters only use 20% of the maximum power allowed in the safest, exempt, risk group will reassure users. In addition, the combination of low transmitter power and high sensitivity receiver will make transmission secure.

The spectrum of white LEDs and the safety limits suggest that, in the future, despite the reduction in the PDE of these SiPMs, operation at wavelengths around 750 nm should be investigated. However, the performance of VLC links in this wavelength range will critically depend upon the availability of absorption filters. In addition, methods of improving the performance of SiPM receivers by reducing their recovery time would be beneficial at all wavelengths.

## APPENDIX A EYE SAFETY CALCULATIONS

The ubiquity of broadband electrically powered light sources, means that they are implicitly assumed to be safe.

However, depending upon their optical power and the distribution of this power across different wavelengths these light sources may cause damage to the eye or the skin.

Any down-link transmitters could be required to operate for long periods and, when in use, a group of them should ensure that an occupied space is fully covered. Since these characteristics are shared by luminaires (light fittings) the most relevant safety standard to apply to VLC transmitters is the IEC 62471:2006 (photobiological safety of lamps and lamp systems) standard. This International Standard specifies the exposure limits, reference measurement techniques and a classification scheme for the evaluation of hazards from all incoherent broadband optical sources in the wavelength range between 200 nm and 3000 nm.

The standard results in a classification of a broad band optical source into one of four different risk groups. Even a momentary or brief exposure to light from a source in risk group 3 (high-risk) may pose a hazard. This definition means that users shouldn't be exposed to any source in this group. A source is risk group 2 (moderate-risk) does not pose a hazard because it will initiate an aversion response. Although, this means that these sources will not cause damage the aversion response will make them unpopular with users. Risk group 1 (low-risk) do not pose a hazard because normal behaviour will limit exposure. This may be an acceptable categorisation for a VLC transmitter. However, potential users are more likely to accept a VLC system that is not a photobiological hazard, and is therefore classified as Risk Group 0 (exempt).

The light from a VLC transmitter will be modulated so rapidly that the relevant section of the standard is the one related to continuous wave lamps. Within this section the classification of a source is based upon seven potential hazards. However, only three of these hazards are relevant to wavelengths between 400 nm and 750 nm. Two of these hazards, blue light and retinal thermal, are related to damage to the retina and their hazard classification is therefore based upon radiance calculations. The blue light small source hazard arises from potential damage to the retina. However, a small source subtends an angle of less than 0.011 rad at the eye. In this work, only sources that subtends angles greater than 0.011 rads are considered and therefore, the only relevant hazards are the blue light and retinal thermal hazards.

For each hazard, the standard provides the exposure limits (EL) defined as the "level of exposure to the eye or skin that is not expected to result in adverse biological effects" [22]. The standard specifies that, for sources other than general lighting sources, the hazard should be evaluated at a distance of 20 cm from the source. Then, since sources can emit a relatively broad band of wavelengths, their risk group for a particular hazard is determined by summing the contributions of each wavelength to that hazard and comparing this to a limit. The overall risk group for the source is then the highest risk group determined from the individual hazards.

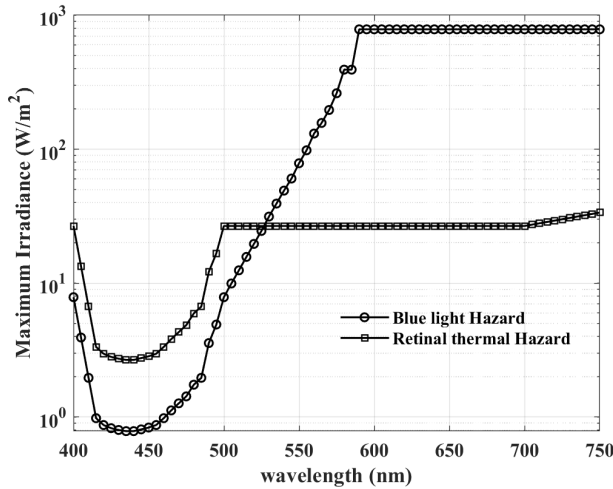


**FIGURE 12.** Eye safe irradiances at a distance of 20 cm from the transmitter as a function of wavelength calculated using  $B(\lambda)$  and  $R(\lambda)$  from [22].

For the blue hazard ( $L_b$ ) following inequality must be true for a source to be exempt.

$$L_b = \sum_{300}^{700} L_\lambda B(\lambda) \Delta\lambda \leq 100 \text{ W/m}^2/\text{sr} \quad (\text{A1})$$

where  $L_\lambda$  is spectral radiance and  $B(\lambda)$  is blue light hazard weighting function. Similarly, for the retinal thermal hazard ( $L_R$ ) the inequality for a source to be exempt is

$$L_R = \sum_{380}^{1400} L_\lambda R(\lambda) \Delta\lambda \leq 28000/\alpha \text{ W/m}^2/\text{sr} \quad (\text{A2})$$

where  $R(\lambda)$  is retinal thermal weighting function and  $\alpha$  is the angular subtense of the source in radians. Assuming that the source has a diameter of 2 cm then  $\alpha$  is 0.1 radians at a distance of 20 cm. This means that the condition for an LED to be exempt

$$L_R = \sum_{380}^{1400} L_\lambda R(\lambda) \Delta\lambda \leq 280000 \text{ W/m}^2/\text{sr} \quad (\text{A3})$$

The band of wavelengths emitted by most VLC transmitters is relatively small compared to the range between 400 nm and 750 nm. The maximum allowed power from an exempt source that has a peak emission wavelength  $\lambda$  can be estimated by assuming that all the power is at this wavelength. Then

$$B(\lambda) L_\lambda(\text{max}) = 100 \text{ Wm}^{-2}\text{sr}^{-1} \quad (\text{A4})$$

and

$$R(\lambda) L_\lambda(\text{max}) = 280000 \text{ Wm}^{-2}\text{sr}^{-1} \quad (\text{A5})$$

Once a maximum allowed radiance value has been determined a solid angle field of view for the eye is required so that the maximum irradiance can be calculated. For the long exposure times associated with the exempt risk group eye movements mean that the angular extent of the field of view,  $\gamma$ , is at least 100 mrad for blue hazard and 11 mrad for

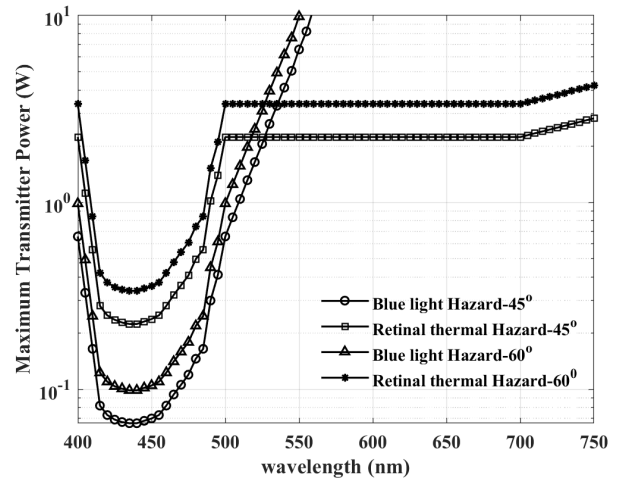


**FIGURE 13.** Eye safe transmitter powers for beams with half angle divergences of 45° and 60° as a function of wavelength calculated using  $B(\lambda)$  and  $R(\lambda)$  from [22].

retinal thermal hazard. The solid angle field of view  $\Gamma$  for blue hazard is then

$$\Gamma = \pi\gamma^2/4 = 7.85 \times 10^{-3} \quad (\text{A6})$$

while for retinal thermal hazard the solid angle FoV is

$$\Gamma = \pi\gamma^2/4 = 9.5 \times 10^{-5} \quad (\text{A7})$$

These two fields of view at the eye mean that A4 becomes

$$B(\lambda) L_\lambda(\text{max}) = 0.785 \text{ Wm}^{-2} \quad (\text{A8})$$

and A5 becomes

$$R(\lambda) L_\lambda(\text{max}) = 26.72 \text{ Wm}^{-2} \quad (\text{A9})$$

The maximum allowed irradiances at 20 cm from the transmitter calculated using A8 and A9 and the values of  $R(\lambda)$  and  $B(\lambda)$  are shown in Fig. 12. These results show that at wavelengths less than 520 nm the allowed irradiance is limited by the blue hazard. Furthermore, the maximum allowed irradiance increases from  $0.98 \text{ Wm}^{-2}$  at 415 nm to  $7.8 \text{ Wm}^{-2}$  at 400 nm. This is because  $B(\lambda)$  decreases from 0.8 at 415 nm to 0.1 at 400 nm.

The maximum allowed irradiances are determined 20 cm from the light source. Consequently, a beam profile is required to convert the maximum irradiances into a maximum allowed power. If the a beam can be represented by a Lambertian profile then [24]:

$$L = \left(\frac{P}{d^2}\right) \left[\frac{m+1}{2\pi}\right] \cos^m(\Phi) \quad (\text{A10})$$

where  $\Phi$  is the angle between transmitter (Tx) and receiver (Rx),  $P$  is the transmitted power,  $d$  is distance between the light source and the eye,  $m = \ln(2)/\ln(\cos \theta_{1/2})$  and  $\theta_{1/2}$  is the transmitter half angle at which the power is half the maximum power [24]. If the beam has a half-angle

of  $45^\circ$  then  $m = 2$ , whilst if the beam has a half angle of  $60^\circ$  then  $m = 1$ . The maximum irradiance occurs when  $\Phi = 0$ , and then the maximum power  $P_{\max}$  is

$$P_{\max} = \frac{2\pi d^2 L_{\max}}{m + 1} \quad (\text{A11})$$

Equations A8-A11 together with the values of  $B(\lambda)$  and  $R(\lambda)$  have been used to calculate the maximum power at each wavelength allowed by the blue and retinal thermal hazards. The results for wavelengths between 400 nm and 750 nm for these two hazards are shown in Figure 13.

The maximum allowed power for both beams shown in Figure 13 increases from 415 nm to 400 nm. Furthermore, this increase is larger than the decrease in the photon detection efficiency of a J series SiPM. The wavelength dependence of the maximum allowed power therefore adds to the advantage of using a wavelength shorter than 420 nm. The central wavelength of laser diodes which could be used as a transmitter means that the maximum allowed power at 405 nm is particularly interesting. For a half angle of  $45^\circ$  the maximum allowed power at 405 nm is 329 mW, whilst the limit for a half angle of  $60^\circ$  is 494 mW. However, the value of  $B(\lambda)$  changes rapidly around 405 nm. Hence, a more conservative estimate, which simplifies the power calculation, and saves power in a deployed system, would be to use the minimum allowed maximum transmitter power for this hazard. This occurs at a wavelength of 440 nm and is 65.8 mW for a half angle of  $45^\circ$  or 98.7 mW for a half angle of  $60^\circ$ .

## ACKNOWLEDGMENT

The research materials supporting this publication can be accessed by contacting [steve.collins@eng.ox.ac.uk](mailto:steve.collins@eng.ox.ac.uk).

## REFERENCES

- R. Bian, I. Tavakkolnia, and H. Haas, "15.73 Gb/s visible light communication with off-the-shelf LEDs," *J. Lightw. Technol.*, vol. 37, no. 10, pp. 2418–2424, May 15, 2019, doi: [10.1109/JLT.2019.2906464](https://doi.org/10.1109/JLT.2019.2906464).
- H. Chun, A. Gomez, C. Quintana, W. Zhang, G. Faulkner, and D. O'Brien, "A wide-area coverage 35 Gb/s visible light communications link for indoor wireless applications," *Sci. Rep.*, vol. 9, no. 1, pp. 4–11, Dec. 2019, doi: [10.1038/s41598-019-41397-6](https://doi.org/10.1038/s41598-019-41397-6).
- L.-Y. Wei, C.-W. Chow, G.-H. Chen, Y. Liu, C.-H. Yeh, and C.-W. Hsu, "Tricolor visible-light laser diodes based visible light communication operated at 40.665 Gbit/s and 2 m free-space transmission," *Opt. Exp.*, vol. 27, no. 18, p. 25072, 2019, doi: [10.1364/oe.27.025072](https://doi.org/10.1364/oe.27.025072).
- C.-Y. Hong, Y.-C. Wu, Y.-H. Lin, Y. Liu, C.-W. Chow, H.-F. Meng, Y.-M. Chang, C.-H. Yeh, K.-L. Hsu, and S.-H. Song, "Visible light positioning (VLP) system using low-cost organic photovoltaic cell (OPVC) for low illumination environments," *Opt. Exp.*, vol. 28, no. 18, pp. 26137–26142, Aug. 2020, doi: [10.1364/OE.399711](https://doi.org/10.1364/OE.399711).
- M. Seminara, T. Nawaz, S. Caputo, L. Mucchi, and J. Catani, "Characterization of field of view in visible light communication systems for intelligent transportation systems," *IEEE Photon. J.*, vol. 12, no. 4, pp. 1–16, Aug. 2020, doi: [10.1109/JPHOT.2020.3005620](https://doi.org/10.1109/JPHOT.2020.3005620).
- Z. Ahmed, R. Singh, W. Ali, G. Faulkner, D. O'Brien, and S. Collins, "A SiPM-based VLC receiver for gigabit communication using OOK modulation," *IEEE Photon. Technol. Lett.*, vol. 32, no. 6, pp. 317–320, Mar. 15, 2020.
- T. Jukić, B. Steindl, and H. Zimmermann, "400  $\mu\text{m}$  diameter APD OEIC in 0.35  $\mu\text{m}$  BiCMOS," *IEEE Photon. Technol. Lett.*, vol. 28, no. 18, pp. 2004–2007, Sep. 15, 2016, doi: [10.1109/LPT.2016.2578979](https://doi.org/10.1109/LPT.2016.2578979).
- Y. Li, M. Safari, R. Henderson, and H. Haas, "Optical OFDM with single-photon avalanche diode," *IEEE Photon. Technol. Lett.*, vol. 27, no. 9, pp. 943–946, May 1, 2015, doi: [10.1109/LPT.2015.2402151](https://doi.org/10.1109/LPT.2015.2402151).
- J. Zhang, L.-H. Si-Ma, B.-Q. Wang, J.-K. Zhang, and Y.-Y. Zhang, "Low-complexity receivers and energy-efficient constellations for SPAD VLC systems," *IEEE Photon. Technol. Lett.*, vol. 28, no. 17, pp. 1799–1802, Sep. 1, 2016, doi: [10.1109/LPT.2016.2572300](https://doi.org/10.1109/LPT.2016.2572300).
- T. Mao, Z. Wang, and Q. Wang, "Receiver design for SPAD-based VLC systems under Poisson–Gaussian mixed noise model," *Opt. Exp.*, vol. 25, no. 2, p. 799, Jan. 2017, doi: [10.1364/oe.25.000799](https://doi.org/10.1364/oe.25.000799).
- C. Wang, H.-Y. Yu, Y.-J. Zhu, T. Wang, and Y.-W. Ji, "Multiple-symbol detection for practical SPAD-based VLC system with experimental proof," in *Proc. IEEE Globecom Workshops (GC Wkshps)*, Dec. 2017, pp. 1–6, doi: [10.1109/GLOCOMW.2017.8269144](https://doi.org/10.1109/GLOCOMW.2017.8269144).
- Y.-D. Zang, J. Zhang, and L.-H. Si-Ma, "Anscombe root DCO-OFDM for SPAD-based visible light communication," *IEEE Photon. J.*, vol. 10, no. 2, pp. 1–9, Apr. 2018, doi: [10.1109/JPHOT.2017.2785798](https://doi.org/10.1109/JPHOT.2017.2785798).
- C. Wang, H.-Y. Yu, Y.-J. Zhu, T. Wang, and Y.-W. Ji, "Multi-LED parallel transmission for long distance underwater VLC system with one SPAD receiver," *Opt. Commun.*, vol. 410, pp. 889–895, Mar. 2018, doi: [10.1016/j.optcom.2017.11.069](https://doi.org/10.1016/j.optcom.2017.11.069).
- A. Eisele and R. Henderson, "185 MHz count rate, 139 dB dynamic range single-photon avalanche diode with active quenching circuit in 130 nm CMOS technology," in *Proc. Int. Image Sensor Workshop*, 2011, pp. 6–8.
- E. Fisher, I. Underwood, and R. Henderson, "A reconfigurable 14-bit 60 GPhoton/s single-photon receiver for visible light communications," in *Proc. Eur. Solid-State Circuits Conf. (ESSCIRC)*, Sep. 2012, pp. 85–88, doi: [10.1109/ESSCIRC.2012.6341262](https://doi.org/10.1109/ESSCIRC.2012.6341262).
- D. Chitnis and S. Collins, "A SPAD-based photon detecting system for optical communications," *J. Lightw. Technol.*, vol. 32, no. 10, pp. 2028–2034, May 15, 2014, doi: [10.1109/JLT.2014.2316972](https://doi.org/10.1109/JLT.2014.2316972).
- O. Almer, D. Tsonev, N. A. W. Dutton, T. A. Abbas, S. Videv, S. Gnechi, H. Haas, and R. K. Henderson, "A SPAD-based visible light communications receiver employing higher order modulation," in *Proc. IEEE Global Commun. Conf. (GLOBECOM)*, Dec. 2014, p. 5, doi: [10.1109/GLOCOM.2014.7417269](https://doi.org/10.1109/GLOCOM.2014.7417269).
- J. Kosman, O. Almer, T. A. Abbas, N. Dutton, R. Walker, S. Videv, K. Moore, H. Haas, and R. Henderson, "A 500 Mb/s –46.1 dBm CMOS SPAD receiver for laser diode visible-light communications," in *IEEE Int. Solid-State Circuits Conf. (ISSCC) Dig. Tech. Papers*, Feb. 2019, pp. 468–470, doi: [10.1109/ISSCC.2019.8662427](https://doi.org/10.1109/ISSCC.2019.8662427).
- W. Matthews, Z. Ahmed, W. Ali, and S. Collins, "A 3.45 Giga-bits/s SiPM-based OOK VLC receiver," *IEEE Photon. Technol. Lett.*, vol. 33, no. 10, pp. 487–490, May 15, 2021, doi: [10.1109/LPT.2021.3069802](https://doi.org/10.1109/LPT.2021.3069802).
- W. Matthews, W. Ali, Z. Ahmed, G. Faulkner, and S. Collins, "Inter-symbol interference and silicon photomultiplier VLC receivers in ambient light," *IEEE Photon. Technol. Lett.*, vol. 33, no. 9, pp. 449–452, May 1, 2021, doi: [10.1109/LPT.2021.3067511](https://doi.org/10.1109/LPT.2021.3067511).
- L. Zhang, X. Tang, C. Sun, Z. Chen, Z. Li, H. Wang, R. Jiang, W. Shi, and A. Zhang, "Over 10 attenuation length gigabits per second underwater wireless optical communication using a silicon photomultiplier (SiPM) based receiver," *Opt. Exp.*, vol. 28, no. 17, p. 24968, Aug. 2020, doi: [10.1364/oe.397942](https://doi.org/10.1364/oe.397942).
- Photobiological Safety of Lamps and Lamp Systems*, Standard IEC 62471:2006/CIES 009:2002, 2006.
- IEEE 802.11-18/1423r8. IEEE P802.11 Wireless LANs TGbb Simulation Scenarios*. Accessed: Mar. 5, 2021. [Online]. Available: <https://mentor.ieee.org/802.11/dcn/18/11-18-1423-08-00bb-tgbb-simulation-scenarios.docx>
- J. M. Kahn and J. R. Barry, "Wireless infrared communications," *Proc. IEEE*, vol. 85, no. 2, pp. 265–298, Feb. 1997, doi: [10.1109/5.554222](https://doi.org/10.1109/5.554222).
- Onsemi. (2020). *J-Series SiPM Sensors Datasheet*. Accessed: Mar. 10, 2020. [Online]. Available: <https://www.onsemi.com/pub/Collateral/MICROJ-SERIES-D.PDF>
- E. Hecht and A. Zajac, *Optics*, vol. 4. San Francisco, CA, USA: Addison-Wesley, 2002.
- L. Zhang, D. Chitnis, H. Chun, S. Rajbhandari, G. Faulkner, D. O'Brien, and S. Collins, "A comparison of APD- and SPAD-based receivers for visible light communications," *J. Lightw. Technol.*, vol. 36, no. 12, pp. 2435–2442, Jun. 15, 2018, doi: [10.1109/JLT.2018.2811180](https://doi.org/10.1109/JLT.2018.2811180).



**WAJAHAT ALI** received the bachelor's degree in electrical engineering degree from Air University, Islamabad, in 2007, and the master's and Ph.D. degrees from Scuola Superiore Sant'Anna, Pisa, in 2013 and 2016, respectively. During his Ph.D., he designed optical wireless communication (OWC) links for high energy physics (HEP) experiments and medical physics application. Since 2019, he has been working as a PDRA with the Department of Engineering Science, University of Oxford. His aim is to design ultra-sensitive optical receivers for visible light communications based on silicon photo-multipliers and fluorescent concentrators.



**GRAHAME FAULKNER** was born in Oxford, U.K., in 1962. He received the B.Sc. degree (Hons.) in physics and microelectronics from Brookes University, Oxford, in 1992. He joined the Department of Engineering Science, University of Oxford, as a Mechanical Technician, in 1986, and became a Research Assistant, in 1996, where he is currently a Senior Researcher and has contributed to over 120 technical publications.



**ZUBAIR AHMED** received the M.Sc. degree in communication electronics from the Linköping University, Sweden, in 2013. He is currently pursuing the D.Phil. degree with the University of Oxford. His thesis is focused on the characterization of single-photon avalanche detectors, such as silicon photomultipliers (SiPMs) and their performance evaluation as an ultra-sensitive visible light communication (VLC) receivers. He is continuing his work on estimating the performance of the SiPM-based VLC receivers in the presence of ambient light.



**WILLIAM MATTHEWS** received the M.Eng. degree in engineering science from the University of Oxford, U.K., in 2019, where he is currently pursuing the D.Phil. degree with the Department of Engineering Science. His thesis is focused on studying the performance of silicon photomultipliers (SiPMs) as an optical wireless communications (OWC) receiver. His current research interest includes performance of SiPM-based VLC receivers when exposed to ambient light.



**STEVE COLLINS** (Member, IEEE) received the B.Sc. degree in theoretical physics from the University of York, York, U.K., in 1982, and the Ph.D. degree from the University of Warwick, Warwick, U.K., in 1986. From 1985 to 1997, he worked with the Defence Research Agency on various topics including the origins of  $1/f$  noise in MOSFETs, imaging sensors, and analogue information processing. Since 1997, he has been with the University of Oxford, Oxford, U.K. Initially he continued his work in microelectronics and investigated applications of wide dynamic range CMOS cameras. His research interest includes significantly improving the performance of VLC receivers.

...